Critical Shear-Wave Velocity Case Histories for Liquefaction Triggering Curves in Gravel

Kyle M. Rollins[1], *Nadia* Salvatore[2#], *Brady R.* Cox[3] and *Tyler* Jackson[3]

[1]*Brigham Young University, Department of Civil and Construction Engineering, 430 Engineering Building, Provo (UT), United States*

[2]*University of Chieti-Pescara, Department of Engineering and Geology, Viale Pindaro, 42, Pescara, Italy*

[3]*Utah State University, Department of Civil and Environmental Engineering, 4110 Old Main Hill, Lofa (UT), United States*

[#]*Corresponding author: nadia.salvatore@phd.unict.it*

ABSTRACT

In 2022, a new set of probabilistic shear wave velocity (V_S) based liquefaction triggering curves was developed for gravelly soil by Rollins et al., using a dataset of 96 liquefaction and 78 no liquefaction case histories from 17 earthquakes in seven countries. Although these curves provide liquefaction assessment based on direct field performance, they suffer from the fact that there are relatively few case histories for high CSR and high V_S values to define the shape of the upper branch of the triggering curves. Thus, we made shear wave velocity measurements at three sites in Valdez, Alaska where liquefaction did not occur in the M_w 9.2 1964 Great Alaska earthquake. The Multi-channel Analysis of Surface Wave (MASW) technique was used to develop several median Vs profiles at each site that account for uncertainty in the experimental dispersion data and inversion parameterizations. V_S-based liquefaction evaluations were then made at each site, using the V_S profiles derived from each solution. Results from previous Dynamic Cone Penetrometer (DPT) tests were then used in selecting the most reasonable velocity interpretation. Based on this V_S profile, the layer most likely to liquefy was selected and used to define V_{S1} and $CSR_{7.5}$ at the middle of this critical layer, obtaining three points of no liquefaction, that could change the shape of the upper branch of the existing V_S-based liquefaction triggering curves. These preliminary results suggest that it might be necessary to shift the triggering curves to the left or steepen their slope to provide better agreement with observed performance.

Keywords: gravel liquefaction; liquefaction triggering curves; shear-wave velocity (V_S).

1. Introduction

The occurrence of liquefaction in gravelly soils under seismic load is well documented in many case histories all over the word (e.g., Rollins et al., 2021; Salvatore et al., 2022). Liquefaction results in economic losses, direct and indirect, deriving from the loss of shear strength in liquefied soils and damage to foundations.

Gravel liquefaction assessment is a big challenge for geologists and engineers, since laboratory testing is expensive due to difficulties in acquiring undisturbed samples in cohesionless soils and in testing large-size particle soils in conventional apparatuses.

Simplified methods for liquefaction assessment in sandy soils based on the Standard Penetration Test (SPT) and the Cone Penetration Test (CPT) are not generally useful in gravelly soils because of the increase of penetration resistance due to the large size of the particles, that might affect the results.

Therefore, simplified methods, using in situ tests such as the Dynamic Penetration Test (DPT) with a 74 mm diameter cone tip, have been developed over the past 10 years (e.g. Cao et al., 2013; Rollins et al., 2021), to provide an inexpensive, easy to use, and accurate method to determine the susceptibility of gravels to liquefaction.

Another alternative which avoids penetrometer interference from large gravel particles are simplified assessment methods based on the shear-waves velocity (V_S) (e.g., Cao et al., 2011; Rollins et al., 2022). The use of this well-known parameter appears to provide a new and interesting frontier in gravel liquefaction assessment.

Even though the V_S parameter is directly related to the small strain shear modulus and is therefore a measure of stiffness at small strains, it can still be useful as an index of liquefaction resistance due to the fact that V_S like liquefaction resistance, is similarly influenced by void ratio, confining stress, stress history, and geological age (Youd et al., 2001).

Furthermore, the use of advanced non-invasive methods of measuring V_S, such as Multichannel Analysis of Surface Waves (MASW), that do not require boreholes and heavy equipment, has made this simplified method for liquefaction assessment cheap and practical when it is not possible to use other in situ tests.

The first attempt at developing probabilistic V_S-based triggering curves for gravelly soils was made by Cao et

al. (2011), considering 30 sites of liquefaction and 17 sites of no liquefaction after the M_W 7.9 2008 Wenchuan earthquake. In 2022, Rollins et al. proposed a new set of curves based on an expanded data set. This data set included 96 liquefaction case histories along with 78 no liquefaction case histories from 17 earthquakes in 7 countries, comprising M_W values ranging from 6.1 to 9.2.

Although these V_S-based liquefaction triggering curves provide liquefaction assessment based on direct field performance, they suffer from the fact that there are relatively few case histories for high CSR and high V_S values to define the shape of the upper branch of the triggering curves.

In an attempt to fill this gap, we have made shear wave velocity measurements using the MASW technique at three sites in Valdez, Alaska where liquefaction did not occur during the M_W 9.2 1964 Great Alaska earthquake.

2. The case study of Valdez site (Alaska)

2.1. Geological setting

The city of Valdez is located in the northern part of the Gulf of Alaska, only 59 km from the epicenter of the M_W 9.2 megathrust earthquake that occurred in Prince William Sound, Alaska, in 1964.

The area is composed of the Upper Cretaceous flysch, underlying softer surficial deposits, consisting of alluvial, colluvial, marine, lacustrine, aeolian, and swamp deposits as shown in Fig. 1.

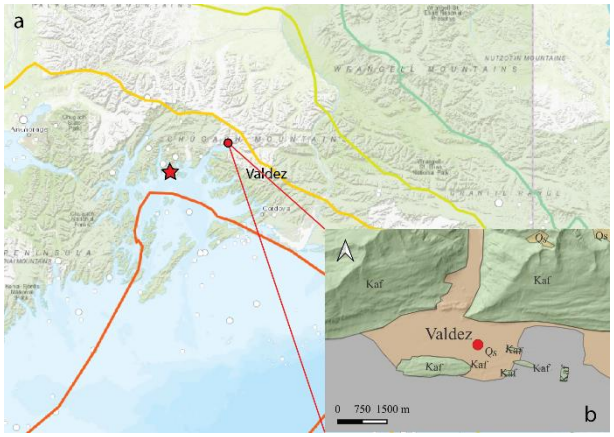

Figure 1. (a) Shake map of the M_W 9.2 Alaska earthquake with the location of Valdez with the respect to the epicenter (red star); contours represent PGA values in %g: orange is the 50%g, yellow is 20%g (modified from https://earthquake.usgs.gov/earthquakes/eventpage/iscgem869809/map?historic-seismicity=true&shakemap-intensity=false). (b) Simplified geological map of Valdez area; Kaf is Chugach flysh, Qs represents surficial deposits while areas covered by water are in grey (modified from: https://alaska.usgs.gov/science/geology/state_map/interactive_map/AKgeologic_map.html)

An extended depression between the main valley wall and a parallel outlying bedrock ridge contains deposits from the Mineral Creek alluvial fan, which is located on the northwestern side of Old Valdez. Many of these deposits consisted of dense sandy gravels. The fan elevation drops from roughly 18 meters above mean sea level at the mountain front down to sea level at the ocean. The outwash delta and Mineral Creek developed broad tidal flats composed of silt, fine sand, and organic muds from the high tidal range.

2.2. Data from previous studies: Standard Penetration Test (SPT) and Dynamic Cone Penetrometer (DPT) tests

After the M_W 9.2 1964 earthquake, the Alaska Highway Department and the US Geological Survey (USGS) made thorough investigations of the Valdez area, highly damaged by the earthquake. As reported by Coulter and Migliaccio (1966), liquefaction and lateral spreading in gravelly soils occurred at the old port of Valdez. Fissures opened up and ejecta consisting of saturated sand and silt erupted from the ground surface due to strong ground shaking. Moreover, the increase in pore pressure at the toe of the submarine slope, combined with other factors, reduced the effective stress, causing a massive submarine landslide.

In contrast, on the northwestern side of the sound, no signs of liquefaction manifestation were observed during the earthquake. In addition, geotechnical investigations consisting of SPT boreholes and tests pits found relatively dense sandy gravel that was not considered liquefiable. Thus, old Valdez was abandoned, and construction of a new Valdez took place at this new site.

We identified three “no liquefaction” gravel case history sites, where boreholes and SPT testing were available from the investigations performed by Shannon & Wilson in connection with the reconstruction after the earthquake. Two of these sites were previously investigated using DPT tests as reported by Rollins et al. (2020) at locations shown in Fig. 2.

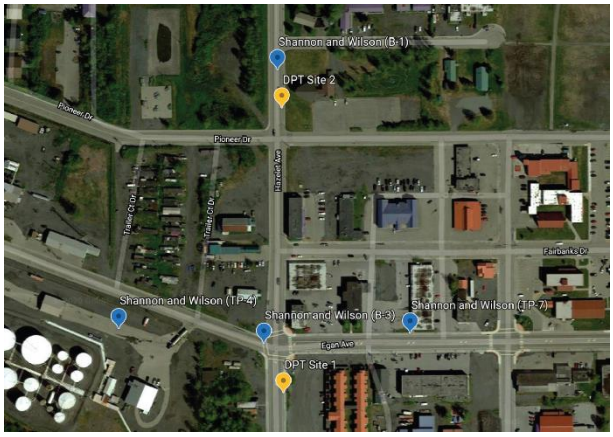

Figure 2. Map of study area in Valdez (Google Earth Pro, imagine 2017); blue dots are boreholes with SPT tests performed by Shannon and Wilson; yellow dots are DPT by Rollins et al. (2020).

The stratigraphic profiles of the three test sites (Shannon and Wilson B-1, B-2, and B-3) indicate that the soil at these sites is mainly composed of medium dense to very dense sandy gravel, with a water table ranging from 3.5 to 6.5 m below the ground surface. Although the soil typically contained 45 to 65% gravel-sized particles, and classified as GM or GW according to the Unified Classification System, they also contained 30% sand. The permeability of sand-gravel mixture with more than 25 to 30% sand typical have Darcy permeability

coefficients more typical of sand than of gravel because the sand fills most of the pore space. As a result the mixture can develop excess pore pressure during earthquake shaking and ultimately liquefy if the relative density is low enough.

2.3. Multi-channel Analysis of Surface Wave (MASW) tests

Three MASW tests were conducted near the three sites investigated by Shannon and Wilson and Rollins et al. (2020), as shown in Fig. (3). The V_S profile can be indirectly estimated using surface-wave dispersion characteristic of the ground (e.g., Kayen et al., 2002), even though it is affected by the uncertainties related both to the limited ability to resolve very thin layers and very short wavelengths, and in inverting the dispersion curve. Moreover, data reliability decreases with depth (Vantassel and Cox, 2021).

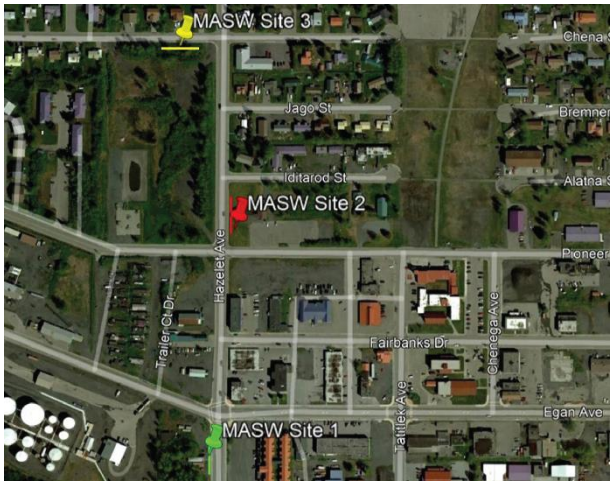

Figure 3. Plan view of the MASW testing sites in Valdez; MASW Site 1 corresponds to Shannon and Wilson B-3, MASW Site 2 with B-1, and MASW Site 3 with B-2.

The dispersion data at Site 1 was interpreted with two different custom layering parameterizations. The first layering parameterization was based on a profile with five layers. This parameterization only allowed a velocity decrease/reversal in V_S in the third layer of the model, so as to fit the flat portion of the dispersion data between 10 – 20 Hz. We refer to this as the "LN = 5 with *Vs* reversal" parameterization. The other layering parameterization was based on a LN = 3 parameterization; however, it did not contain a velocity reversal. Rather, the flat part in the dispersion data was fit using a thicker layer of intermediate V_S. This parameterization is referred to as the "LN = 3 no V_S reversal" parameterization (Fig. 4 Site 1).

The dispersion data at Site 2 was interpreted with three different layering parameterizations based on the layer number (LN) approach, wherein subsurface models with four, six, and eight potential layers (i.e., LN = 4, LN = 6, and LN = 8) were considered as a means to account for epistemic uncertainty (Fig. 4 Site 2).

The dispersion data at Site 3 was interpreted with three different layering parameterizations based on the layering number (LN) approach, wherein subsurface models with four, six, and eight potential layers (i.e., LN = 4, LN = 6, and LN = 8) were considered as a means to account for epistemic uncertainty (Fig. 4 Site 3). Inversion results for each site are based on a fundamental mode interpretation/inversion of the experimental Raleigh wave dispersion data. Fig. 4 shows the medians of the 100 best: (a) theoretical dispersion curves relative to the experimental dispersion data, and (b) V_S profiles shown to a depth of 30 m for each site. The dispersion misfit values for each inversion parameterization are indicated by brackets for various frequencies.

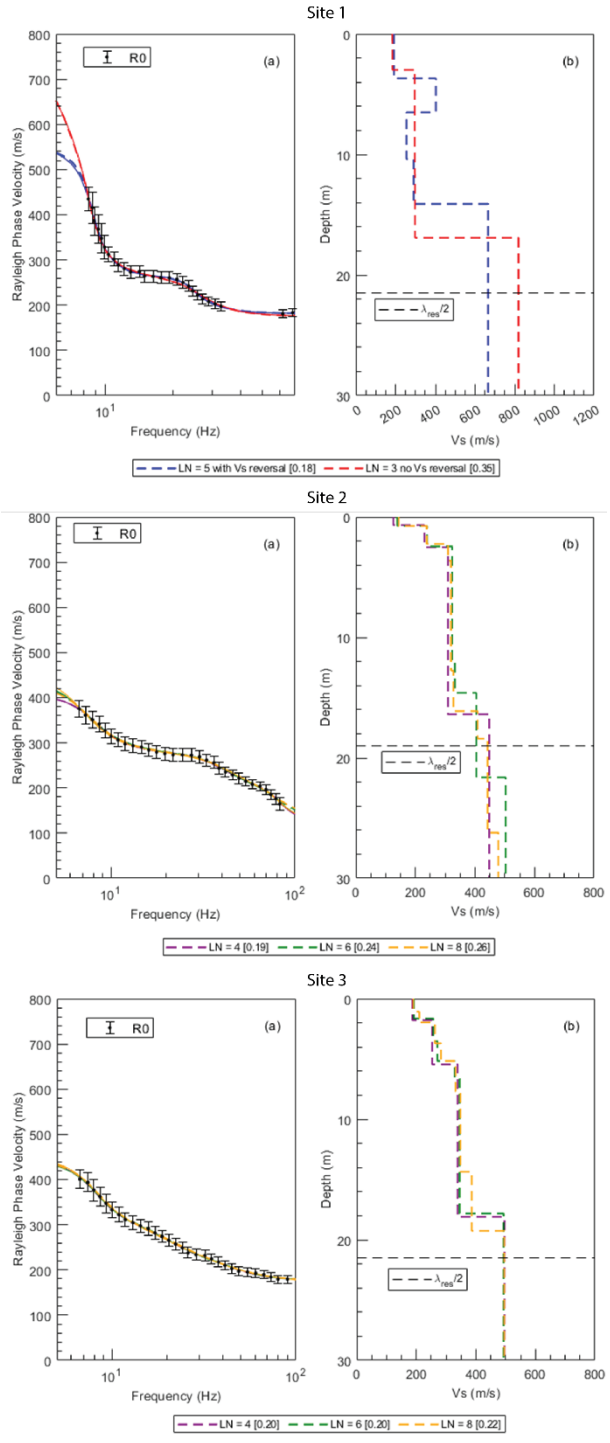

Figure 4. (a) Mean dispersion curves and (b) interpreted *Vs* profiles from inversions of MASW results at Site 1, Site 2, and Site 3 at Valdez.

For Site 1, plots are presented for LN=3 and LN=5 in Fig. 4 (a). The array resolution depth limit ($d_{res} = \lambda_{res}/2$) is

shown at 21.5 m. Inversion results for Site 2 are shown for LN = 4, LN = 6, LN = 8 in Fig. 4 (b). The array resolution depth limit ($d_{res} = \lambda_{res}/2$) is shown at 19 m. Inversion results for Site 3 are shown in Fig. 4 (c) for LN = 4, LN = 6, LN = 8. The array resolution depth limit ($d_{res} = \lambda_{res}/2$) is shown at 21.5 m.

3. Methods for computing cyclic stress ratio (CRR) and liquefaction factor of safety at sites in Valdez, Alaska

In this study, the liquefaction resistance of the gravel sites in Valdez was evaluated using both the shear wave velocity (V_S) and the Dynamic Cone Penetration (DPT) blow count for comparison purposes.

3.1. DPT-Based Liquefaction Assessment

The DPT was developed in China in the early 1950s to reduce the effect of gravel size particles on the penetration resistance. DPT equipment consists of a 120 kg hammer, which is dropped from a 1 m height onto a 60 mm diameter drill rod with a solid cone tip having a diameter of 74 mm. The hammer energy is approximately 2.5 times greater than for the SPT hammer energy.

During the test, the cone is driven continuously into the ground and the number of blows required to penetrate each 10 cm is recorded, but multiplied by three to give the equivalent blow count for a 30 cm interval, consistent with the SPT. The raw DPT blow count is then corrected considering the energy transferred from the hammer to the rods to obtain the blow count, N_{120} (Cao et al., 2013; Rollins et al., 2021).

As suggested by Cao et al. (2013), an overburden correction factor is applied to the N_{120}, to obtain the normalized N'_{120} value using the equation:

$$N'_{120} = N_{120} C_N \quad (1)$$

where

$$C_N = (100/\sigma'_{v0})^{0.5} \leq 1.7 \quad (2)$$

and σ'_{v0} is the vertical effective stress in kN/m^2 (Youd et al., 2001). The Cyclic Stress Ratio (CSR) induced by the earthquake can be calculated as originally proposed by Seed and Idriss (1971) using the equation:

$$CSR = 0.65(a_{max}/g)(\sigma_{v0}/\sigma'_{v0})r_d \quad (3)$$

where a_{max} is the peak ground acceleration, σ_{v0} is the initial vertical stress and r_d is a depth reduction factor as defined in Idriss et al. (1999). To make the data comparable regardless of the earthquake, M_W is standardized to the value of 7.5 using the equation:

$$CSR_{7.5} = CSR/MSF \quad (4)$$

Where MSF is the Magnitude Scaling Factor given by the equation

$$MSF = 7.258\exp(-0.264M_W) \quad (5)$$

as proposed by Rollins et al. (2021) for DPT data.
Using N'_{120}, the probability of liquefaction P_L can also be calculated as indicated in Rollins et al. (2021), following the equation:

$$P_L = \frac{1}{1 + \exp(-0.008N'^3_{120} + 1.32M_W + 5.2\ln CSR)} \quad (6)$$

From this, the Cyclic Resistance Ratio (CRR) can be considered as:

$$CRR = exp\left[\frac{0.008N'^3_{120} - 1.32M_W - \ln\left(\frac{1-P_L}{P_L}\right)}{5.2}\right] \quad (7)$$

The factor of safety against liquefaction (FS) can then be calculated using the equation.

$$FS = CRR/CSR_{7.5} \quad (8)$$

originally developed for sand by Seed and Idriss (1971).

3.2. V_S-based Liquefaction Assessment

For the three sandy gravel sites in Valdez, the V_S interpreted from the MASW measurements was corrected for overburden pressure to obtain the normalized shear wave velocity (V_{S1}) using the equation proposed by Youd et al. (2001):

$$V_{S1} = V_S(100/\sigma'_{v0})^{0.25} \quad (9)$$

To preserve the constant velocity profiles obtained from the inversion process, the V_{S1} correction was simply employed at the mid-height of each layer.

The CSR was calculated as in Eq. (3) and standardized to a M_W 7.5 event as in Eq. (4) to obtain the $CSR_{7.5}$. However, for the V_{S1}-based approach the MSF is calculated as in Rollins et al. (2022):

$$MSF = 10.667exp(-0316M_W) \quad (10)$$

Plots of the V_{S1} and the $CSR_{7.5}$ for each of the three gravel site in Valdez are provided in Fig. 7, along with the location of the critical layers. The P_L based on the V_{S1} can be calculated as indicated in Rollins et al. (2022), following the equation:

$$P_L = \frac{1}{1 + \exp(-1.6M_W - 4.95\ln CSR + 3.88x10^{-7}V^3_{S1})} \quad (11)$$

From this, the CRR can be defined as:

$$CRR = exp\left[\frac{3.88x10^{-7}V^3_{S1} - 1.6M_W - \ln\left(\frac{1-P_L}{P_L}\right)}{4.95}\right] \quad (12)$$

Likewise, the factor of safety against liquefaction was evaluated for each profile using Eq. (8).

The overall susceptivity of a soil profile to liquefaction can be estimated using the Liquefaction Potential Index (LPI) proposed by Iwasaki et al. (1978), as in equation:

$$LPI = \int_0^{20} F(z)w(z)\Delta z \quad (13)$$

where

$$w(z) = 10 - 0.5z \quad (14)$$

$$F(z) = 1 - FS \; if \; FS \leq 1 \; ; F(z) = 0 \; if \; FS > 1 \quad (15)$$

4. Results from DPT and Vs based analyses

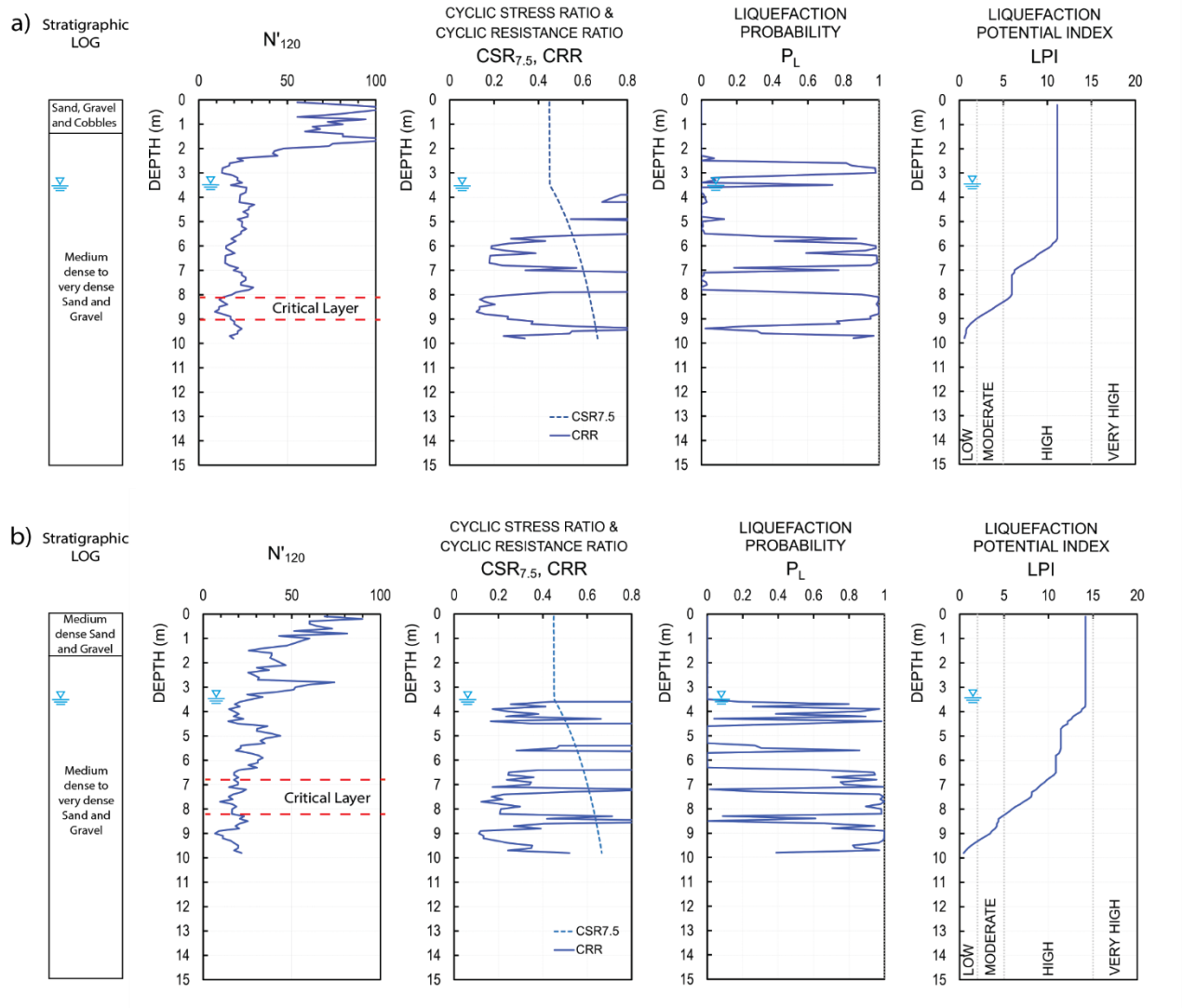

Figure 5. Plots of N'_{120} and critical layers along with DPT-based CRR, $CSR_{7.5}$, P_L probability of liquefaction and LPIs using the simplified method by Rollins et al. (2021) at (a) Site 1and (b) Site 2 in Valdez, Alaska for the 1964 M_W 9.2 Great Alaskan Earthquake.

Plots of N'_{120} vs. depth for Sites 1 and 2 in Valdez are plotted in Fig. 5 along with plots of the DPT-based $CSR_{7.5}/CRR$, FS, and LPI vs. depth. The CRR and FS values were computed using a 15% probability of liquefaction using Eq. (6) and (7), respectively. Using a conservative P_L of 15% rather than 50%, a zone from 5.5 to 7 m would be predicted to liquefy even though no surface manifestation of liquefaction was observed at these sites.

Based on the plots of N'_{120} versus depth and $CSR_{7.5}$ versus depth, the critical layer for each site in Valdez was selected as the gravel layer that was most likely to trigger and manifest liquefaction at the ground surface (Cao et al. 2013; Dhakal et al. 2018). Typically, this was the gravelly layer corresponding to the lowest average N'_{120} value below the water table relative to the $CSR_{7.5}$. Any cohesive layers were excluded from consideration. The critical layer was selected having a thickness of about one meter or more to provide a representative average N'_{120} value which is less affected by thin peaks or troughs (Boulanger and Idriss 2014). For the two sites in Valdez, the critical layer at each site is also identified in Fig. 5.

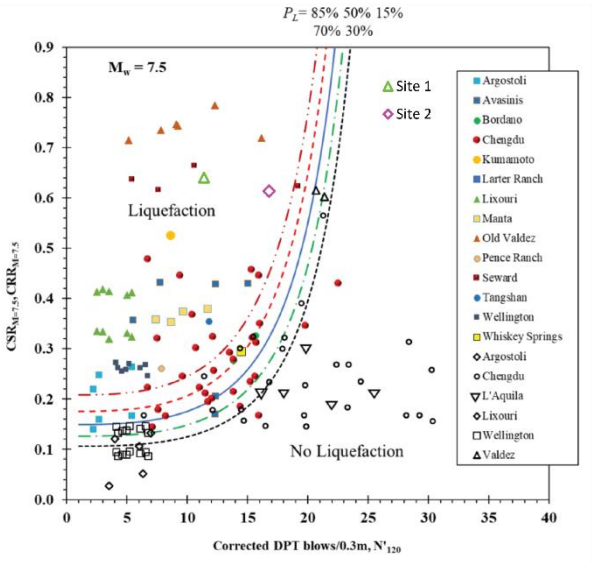

Figure 6. Plot of $CSR_{7.5}$ and N'_{120} showing no-liquefaction points from Valdez relative to the triggering curves by Rollins et al. (2021)

The two $CSR_{7.5}$ and N'_{120} data pairs are plotted in Fig. 6 relative to the probabilistic DPT-based liquefaction triggering curves proposed by Rollins et al. (2021). Critical layers for the two sandy gravel sites in Valdez have a probability of liquefaction based on the DPT-based triggering curves higher than 85%. In correspondence with the DPT analyses, liquefaction assessment using the V_{S1}-based simplified method proposed by Rollins et al. (2022) was performed at each site using all the velocity inversion solutions obtained from MASW acquisitions

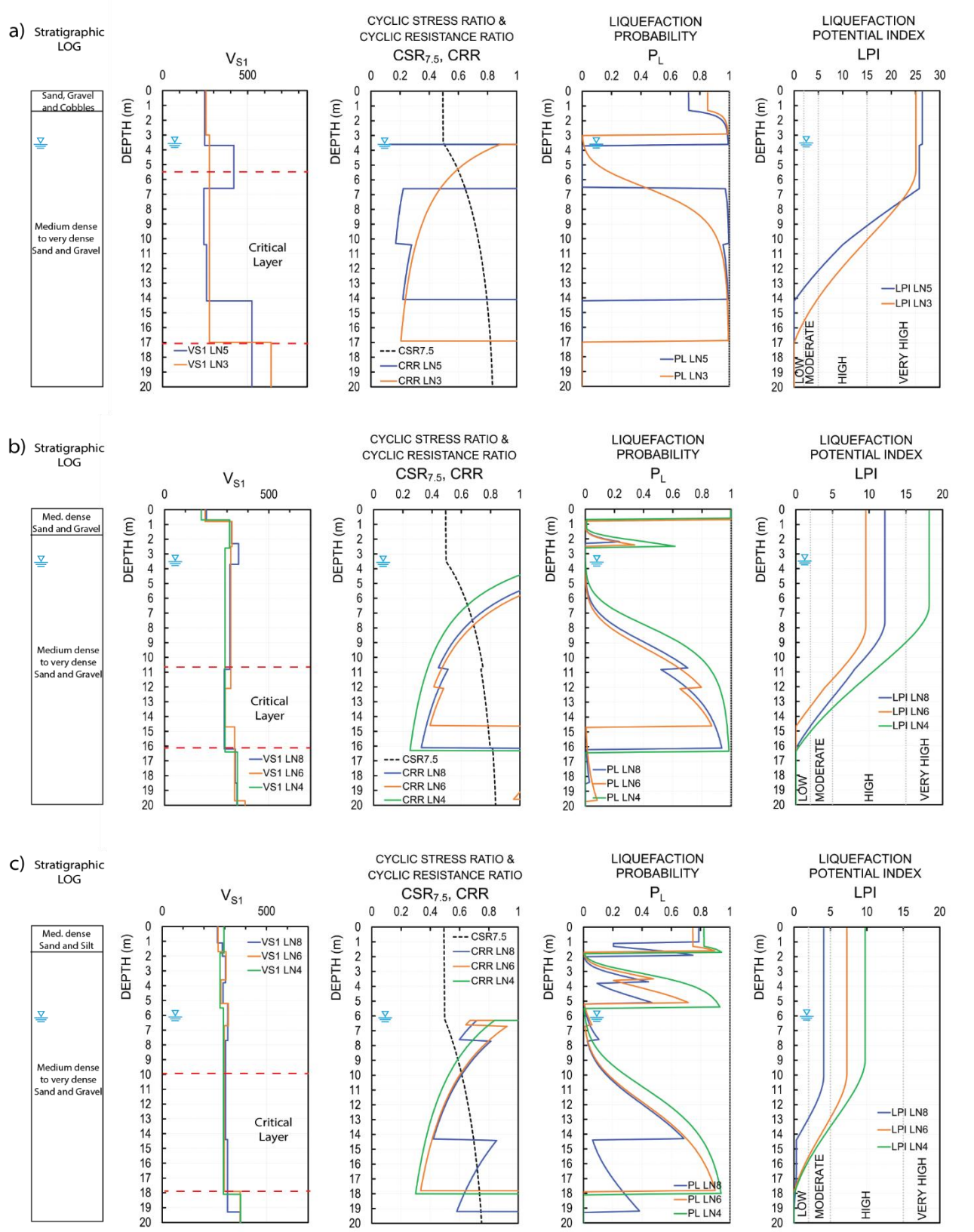

Figure 7. Plots of V_{S1} and critical layers along with V_{S1}-based CRR, $CSR_{7.5}$, P_L probability of liquefaction and LPIs using the simplified method by Rollins et al. (2022) at (a) Site 1, (b) Site 2 and (c) Site 3 in Valdez, Alaska for the 1964 M_W 9.2 Great Alaskan Earthquake.

The most reasonable velocity interpretation from velocity inversion in Fig. 4 for each site was selected by considering the solution with the LPI value closest to the LPI obtained with the DPT analysis. For Site 3, where no DPT test was performed, we based the selection on a stratigraphic criteria, considering the most similar condition in Site 2.

Plots of V_{S1} vs. depth for Sites 1, 2 and 3 in Valdez are plotted in Fig. 7 along with plots of the V_S-based $CSR_{7.5}/CRR$, FS, and LPI vs. depth. The CRR and FS values were computed using a 15% probability of liquefaction using Eq. (10) and (7), respectively. Using a conservative P_L of 15% rather than 50%, a zones of over 2-m thick would be predicted to liquefy at these sites even though no surface manifestation of liquefaction was observed at these sites.

Using the same procedure as described for the DPT soundings, the critical layer, defined as the layer most likely to liquefy, was selected for solutions LN3 at Site 1, LN8 at Site 2 and LN6 at Site 3. It appears important to observe that the critical depths for the V_S-based plots of Site 1 and 2 are deeper than the DPT, and that could be the reason why the $CSR_{7.5}$ are so low in that case (Fig. 6).

The critical layers for V_S-based are also plotted in Fig. 7. The V_{S1} and $CSR_{7.5}$ values, taken at the middle of each of these critical layers, provide three pairs of $CSR_{7.5}$ and V_{S1} values for these three "no liquefaction" case histories.

The $CSR_{7.5}$ and V_{S1} data pairs are plotted in Fig. 8 relative to the probabilistic V_{S1}-based liquefaction triggering curves proposed by Rollins et al. (2022).

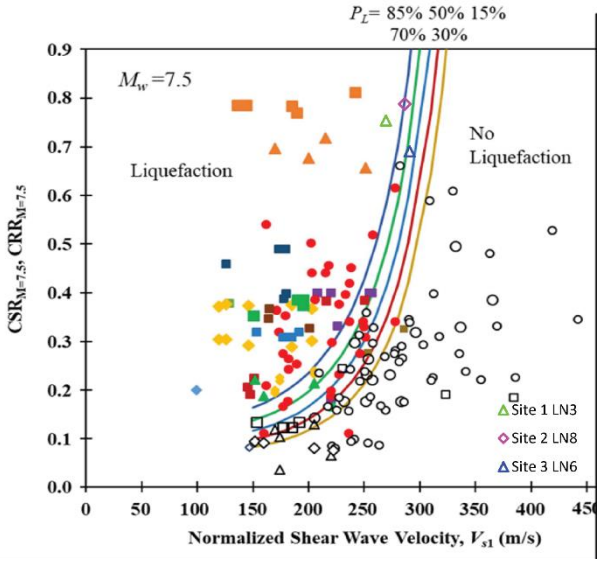

Figure 8. Plot of $CSR_{7.5}$ and V_{S1} showing no-liquefaction point from Valdez relative to the triggering curves by Rollins et al. (2022).

Critical layers for two of the sandy gravel sites in Valdez have a 50 to 85% probability of liquefaction based on the V_S-based triggering curves. In addition, a third case history has a liquefaction probability higher than 85%. These critical case histories have the potential to shift the triggering curve boundaries for the upper branch of the curve. These results also point out the necessity of obtaining additional case histories in the high $CSR_{7.5}$ and V_{S1} range that often controls the design of critical infrastructure.

5. Conclusions

Based on the results of the field and lab testing, the following conclusions have been developed:

1. The sandy gravels at the sites in Valdez typically contained more than 30% sand. This sand content had the effect of reducing the permeability so that the sand-gravel mixture could generate excess pore pressures and potentially liquefy.
2. Although there is no evidence that the sandy gravel in Valdez liquefied in the M_W 9.2 Great Alaskan Earthquake in 1964, liquefaction evaluations based on the dynamic cone penetration test (DPT) blow count indicate that probability of liquefaction was higher than 85%. These evaluations, based on the DPT-based triggering curve proposed by Rollins et al. (2021), indicate that these data points are critical in establishing the shape of the upper branch of the triggering curves.
3. As was observed with the DPT test results, the V_S test results at the two sand gravel sites in Valdez have 50 to 85% probability of liquefaction based on the V_S-based triggering curves proposed by Rollins et al. (2022). In addition, a third case history has a liquefaction probability higher than 85%. These critical case histories have the potential to shift the triggering curve boundaries for the upper branch of the curve.
4. Considering the sparse set of case histories available for high $CSR_{7.5}/V_S$/DPT blow counts, additional case histories in this critical range should be identified and investigated.

Acknowledgements

Funding for this study was provided by a grant from the US Geological Survey under the earthquake hazard reduction program. This support is gratefully acknowledged although the conclusion and opinions expressed in this paper are not necessarily those of the sponsor.

References

Boulanger, R.W, Idriss, I.M. 2014. « CPT and SPT based liquefaction triggering procedures." Center for Geotechnical Modeling, Dept. of Civil and Environ. Engrg. Univ. of Calif.-Davis; p. 134. Report No. UCD/CGM-14/01.

Cao, Z., Youd, T. L., Yuan, X. 2011. "Gravelly soils that liquefied during 2008 Wenchuan, China Earthquake, Ms=8.0." Soil Dyn. Earthq. Eng., 31 (8). https://doi.org/10.1016/j.soildyn.2011.04.001

Cao, Z., Youd, T. L., Yuan, X. 2013. "Chinese Dynamic Penetration Test for Liquefaction Evaluation in Gravelly Soils." J. Geotech. Geoenvironmental Eng., 139 (8). https://doi.org/10.1061/(ASCE)GT.1943-5606.0000857

Coulter, H.W., Migliaccio, R.R. 1966. "Effects of the Earthquake of March 27, 1964 at Valdez, Alaska" The

Alaska Earthquake Series, Geological Survey Professional Paper 542-C, Washington, D.C.

Dhakal, R., Cubrinovski, M., Bray, J., de la Torre, C. 2020. “Liquefaction assessment of reclaimed land at Centreport, Wellington.” Bull. N.Z. Soc. Earthq. Eng. 53(1), 1–12.

Idriss, I. M. 1999. “An update to the Seed-Idriss simplified procedure for evaluating liquefaction potential”. In Proceedings, TRB Workshop on New Approaches to Liquefaction, Publication No. FHWA-RD-99-165, Federal Highway Administration

Iwasaki, T., Tatsuoka, F., Tokida, K., Yasuda, S. 1978. “A practical method for assessing soil liquefaction potential based on case studies at various sites in Japan”. Second international Conference on Microzonation for Safer Construction Research and Application.

Kayen, R., Tanaka, Y., Cetin, O., Hayashi K., Minasian, D., Seed, R.B., Suzuki, Y., Tokimatsu, K. 2002. “Surface Wave Investigation and Analysis Earthquake-Induced Liquefaction Sites in Asia”. AGU Fall Meeting Abstracts 2002

Rollins, K.M., Roy, J., Amoroso S., Linton N. 2020. “Evaluation of the Dynamic Cone Penetration Test (DPT) for liquefaction triggering at gravel sites in Alaska and Italy”. In 6th International Conference on Geotechnical and Geophysical Site Characterization. https://doi.org/10.53243/ISC2020-230

Rollins, K.M, Roy, J., Athanasopoulos-Zekkos, A., Zekkos, D., Amoroso, S., Cao, Z. 2021. “A New Dynamic Cone Penetration Test-Based Procedure for Liquefaction Triggering Assessment of Gravelly Soils”, J. Geotech. Geoenviromental Eng., 147 (12), https://doi.org/10.1061/(ASCE)GT.1943-5606.0002686

Rollins, K.M., Roy, J., Athanasopoulos-Zekkos, A., Zekkos, D., Amoroso, S., Cao, Z., Milana, G., Vassallo, M., Di Giulio, G. 2022. “A New V_S-Based Procedure Liquefaction-Triggering Procedure for Gravelly Soils”, J. Geotech. Geoenviromental Eng., 148 (6), https://doi.org/10.1061/(ASCE)GT.1943-5606.0002784

Salvatore, N., Pizzi, A., Rollins, M.K., Pagliaroli, A., Amoroso, S. 2022. “Liquefaction assessment of gravelly soils: the role of in situ and laboratory geotechnical tests through the case study of the Sulmona basin (Central Italy)”, Ital. J. Geosci., 141 (2), https://doi.org/10.3301/IJG.2022.18

Seed, H.B., Idriss, I. 1971. “Simplified Procedure for Evaluating Soil Liquefaction Potential”. J. Soil Mech. Found. (97)9 https://doi.org/10.1061/JSFEAQ.000166

Vantassel, J.P., Cox, B.R. 2021. “A procedure for developing uncertainty-consistent V_S profiles from inversion of surface wave dispersion data”. Soil Dyn. Earthq. Eng., 145, https://doi.org/10.1016/j.soildyn.2021.106622

Youd, T.L., Idriss, I.M., Andrus, R.D., Arango, I., Castro, G., Christian, J.T., Dobry, R., Finn, W.D.L., Harder, L.F., Hynes, M.E., Ishihara, K., Koester, J.P., Liao, S.S.C., Marcuson, W.F., Martin, G.R., Mitchell, J.K., Moriwari, Y., Power, M.S., Robertson, P.K., Seed, R.B., Stokoe, K.H. 2001. “Liquefaction resistance of soils: summary report from the 1996 NCEER and 1998 NCEER/NSF workshops on evaluation of liquefaction resistance of soils”. J. Geotech. and Geoenviron. Eng., 127 (10), 817-833. https://doi.org/10.1061/(ASCE)1090-0241(2001)127:10(817)